

## Functional Heme Binding to the Intrinsically Disordered C-Terminal Region of Bach1, a Transcriptional Repressor

Kei Segawa,<sup>1,2</sup> Miki Watanabe-Matsui,<sup>3,4</sup> Toshitaka Matsui,<sup>5</sup> Kazuhiko Igarashi<sup>3</sup>  
and Kazutaka Murayama<sup>1,6</sup>

<sup>1</sup>Division of Biomedical Measurements and Diagnostics, Graduate School of Biomedical Engineering, Tohoku University, Sendai, Miyagi, Japan

<sup>2</sup>Pharmaceutical Discovery Research Laboratories, Teijin Pharma Limited, Tokyo, Japan

<sup>3</sup>Department of Biochemistry, Graduate School of Medicine, Tohoku University, Sendai, Miyagi, Japan

<sup>4</sup>Japan Society for the Promotion of Science (JSPS), Tokyo, Japan

<sup>5</sup>Institute of Multidisciplinary Research for Advanced Materials, Tohoku University, Sendai, Miyagi, Japan

<sup>6</sup>Laboratory for Protein Functional and Structural Biology, RIKEN Center for Biosystems Dynamics Research, Yokohama, Kanagawa, Japan

Heme is one of the key factors involved in the oxidative stress response of cells. The transcriptional repressor Bach1 plays an important role in this response through its heme-binding activity. Heme inhibits the transcriptional-repressor activity of Bach1, and can occur in two binding modes: 5- and 6-coordinated binding. The Cys-Pro (CP) motif has been determined to be the heme-binding motif of Bach family proteins. The sequence of Bach1 includes six CP motifs, and four CP motifs are functional. With the aim of elucidating the molecular mechanism of heme-Bach1 regulation, we conducted biophysical analyses focusing on the C-terminal region of mouse Bach1 (residues 631-739) which is located after the bZip domain and includes one functional CP motif. UV-Vis spectroscopy indicated that the CP motif binds heme via 5-coordinated bond. A mutant, which included a cysteine to alanine substitution at the CP motif, did not show 5-coordination, suggesting that this binding mode is specific to the CP motif. Surface plasmon resonance revealed that the binding affinity and stoichiometry of heme with the Bach1 C-terminal region were  $K_D = 1.37 \times 10^{-5}$  M and 2.3, respectively. The circular dichroism spectrum in the near-UV region exhibited peaks for heme binding to the CP motif. No significant spectral shifts were observed in the far-UV region when samples with and without heme were compared. Therefore, disorder-ordered transition such as “coupled folding and binding” is not involved in the Bach1-heme system. Consequently, the heme response of this C-terminal region is accomplished by disorder-disorder conformational alteration.

**Keywords:** circular dichroism spectroscopy; Cys-Pro motif; heme; intrinsically disordered protein; protein conformation

Tohoku J. Exp. Med., 2019 March, 247 (3), 153-159. © 2019 Tohoku University Medical Press

### Introduction

The transcriptional repressor Bach1 binds to Maf recognition element (MARE) sequences within the enhancer and promoter regions of oxidative stress-related genes such as heme oxygenase (HO)-1, and genes involved in ferritin or heme metabolism (Hintze et al. 2007). Bach1 is inactivated by heme or oxidative stress. When this occurs, transcription of target genes is induced by binding of the Nrf2/Maf hetero dimer to the MARE sequence which is now available (Sun et al. 2002; Ishikawa et al. 2005). The HO-1 gene product is the rate-limiting enzyme of heme metabolism. Carbon monoxide that is produced during heme degradation has strong anti-inflammatory actions, and its

metabolite bilirubin has antioxidant activity (Chung et al. 2009). These properties suppress apoptosis and inflammatory cytokine production. Thus, inhibition of Bach1 is expected to induce HO-1 expression to protect cells. Such an inhibitor represents a potential drug target. Previous studies on Bach1 knock-out mice have demonstrated the acceleration of biological defense following Bach1 inhibition (Yano et al. 2006; Yamada et al. 2008). Yano et al. (2006) reported that Bach1 knock-out mice over-expressed HO-1, and the tissue-protective effect of this enzyme prevented tissue injury in a myocardial ischemia reperfusion model.

The Bach family proteins Bach1 and Bach2 possess Broad-Complex, Tramtrack and Bric a brac (BTB) (Ito et

Received January 28, 2019; revised and accepted February 19, 2019. Published online March 9, 2019; doi: 10.1620/tjem.247.153.

Correspondence: Kazutaka Murayama, Division of Biomedical Measurements and Diagnostics, Graduate School of Biomedical Engineering, Tohoku University, 2-1 Seiryomachi, Aoba-ku, Sendai, Miyagi 980-8575, Japan.  
e-mail: kazutaka.murayama.d4@tohoku.ac.jp

al. 2009; Rosbrook et al. 2012) and Basic Leucine Zipper (bZip) domains, separated by long unstructured sequences. The Bach proteins contain a conserved Cys-Pro (CP) motif, which has been identified as the heme binding site (Lathrop and Timko 1993; Zhang and Guarente 1995). There are two heme binding modes for Bach proteins: 5- and 6-coordination (Hira et al. 2007; Watanabe-Matsui et al. 2011; Igarashi and Watanabe-Matsui 2014). Of these binding modes, the axial ligand of 5-coordination is specific to the cysteine in the CP motif. The two modes of heme binding play significant roles in regulating the intrinsically disordered states of the proteins, as the CP motifs are located in the unstructured regions. Our previous studies of Bach2 revealed that when heme binding occurs in the intrinsically disordered region, the conformation of the region is altered (Watanabe-Matsui et al. 2015; Suenaga et al. 2016). However, the Bach2 heme-binding region was found to be an insertion part in comparison between Bach1 and Bach2. The sequence of Bach1 includes a total of six CP motifs (CP1-CP6). The positions of these CP motifs are conserved between mouse and human orthologues, although human Bach1 contains an extra CP motif at the Cys140. Of these, the four CP motifs in the C-terminal side (CP3-CP6) are functional (Suzuki et al. 2004; Hira et al. 2007). The CP motif located in the C-terminal moiety of the bZip domain (CP6) is thought to be the site of heme binding (Fig. 1), and the corresponding region of Bach2 (after the bZip domain) also includes one CP motif. However, the molecular mechanisms of heme binding and response are still unclear. An understanding of the heme response of Bach1 is essential to elucidate the molecular mechanisms involved in regulation of the heme-Bach1 system.

Here, we report the biophysical characterization of Bach1. This study focused on the C-terminal heme-binding region (631-739), which includes one functional CP motif. The heme binding and response of Bach1 were analyzed with spectroscopic measurements. The results suggested

that biophysical response of the Bach1 C-terminal region is a disordered-to-disordered alternation.

## Materials and Methods

### Preparation of Bach1 samples

The mouse Bach1 DNA fragment encoding residues 631-739 (named “Bach1HBR-C”; Bach1 heme-binding region, C-terminal) (Fig. 1) was cloned into a pGEX-6P-1 vector (GE Healthcare; Buckinghamshire, England). A mutant was prepared, in which Cys649 was substituted with alanine (named “mCP”). *Escherichia coli* BL21 cells (BioDynamics Laboratory Inc., Tokyo, Japan), transformed with the expression construct for the GST-Bach1HBR-C fusion protein, were grown in Luria Broth medium containing 2% glucose and 100  $\mu$ g/mL ampicillin at 37°C until the OD<sub>600</sub> reached 0.6. After the addition of 1 mM isopropyl  $\beta$ -D-1-thiogalactopyranoside (IPTG), cultures were incubated at 16°C overnight. Cells were suspended in lysis buffer (50 mM Tris-HCl, pH 8.0, 150 mM NaCl, 2 mM tris[2-carboxyethyl]phosphine [TCEP], 0.1% [w/v] n-dodecyl  $\beta$ -D-maltopyranoside, and protease inhibitor cocktail), sonicated on ice and centrifuged at 12,000  $\times$  g for 20 min. The supernatant was incubated with Glutathione Sepharose 4B (GE Healthcare) for 2 h at 4°C with gentle rotation. The resin was then washed with wash buffer (50 mM Tris-HCl, pH 8.0, 150 mM NaCl, 50% glycerol), and incubated with elution buffer (20 mM Tris-HCl, pH 8.0, 100 mM NaCl, 2 mM TCEP, 20  $\mu$ L/mL Turbo3C protease (FUJIFILM Wako Pure Chemical, Osaka, Japan)) with gentle rotation overnight at 4°C. Supernatant containing the eluted protein was applied to a Mono Q column (GE Healthcare) that had been pre-equilibrated with 20 mM Tris-HCl, pH 8.0, 2 mM TCEP. A sodium chloride linear gradient was used to elute the Mono Q-bound fractions. The fraction containing the protein was concentrated to 2-4 mg/mL using a Vivaspin spin column (GE Healthcare) and applied to a Superdex 75 Increase column (GE Healthcare) that had been pre-equilibrated with 20 mM 4-(2-hydroxyethyl)-1-piperazineethanesulfonic acid (HEPES), pH 7.5, 50 mM NaCl, 2 mM TCEP. Protein solutions were typically concentrated to 1-2 mg/mL.

The 25-amino-acid peptide of Bach1 corresponding to residues 634-658 (Fig. 1) was designed to include the heme-binding CP motif and synthesized by Greiner Bio-One (Tokyo, Japan). A stock solution

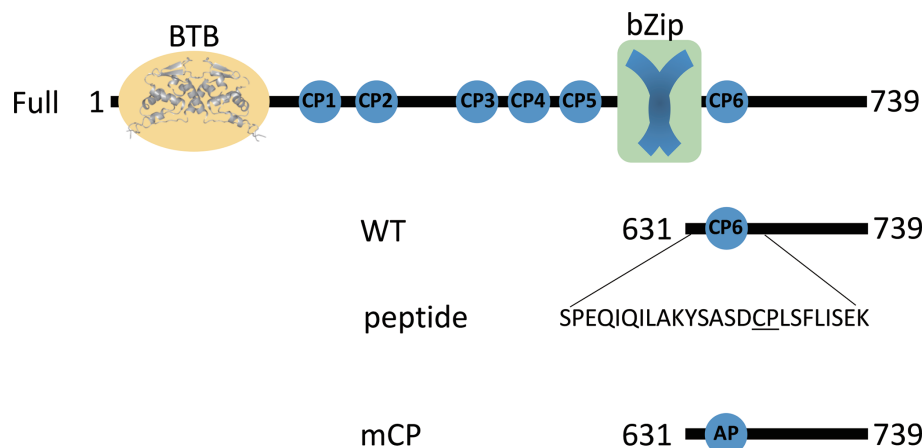


Fig. 1. Diagrammatic representation of the Bach1 constructs and synthesized peptides.

Cysteine-proline motifs are depicted by circle.

BTB, Broad-Complex, Tramtrack and Bric a brac; bZip, Basic Leucine Zipper; mCP, Cys649 to alanine mutated construct; CP, cysteine-proline; WT, wild type.

was prepared by dissolving the peptide in distilled water and adjusting to 1 mg/mL.

#### Circular dichroism and dynamic light scattering measurements

Protein samples were diluted to 8.6  $\mu$ M (0.1 mg/mL) in 10 mM HEPES, pH 7.5, 50 mM NaCl, 2 mM TCEP. Circular dichroism (CD) spectra were measured with or without 8.6  $\mu$ M heme (hemin, Sigma-Aldrich, St. Louis, MO, USA) using a J-805 spectrometer (Jasco, Tokyo, Japan) in the far-UV region (200–250 nm) with a 1 mm path-length cuvette. Spectra were averaged over four scans. Measurements were taken from 20 to 60°C with 5°C increment steps. Measurements in the near-UV region (250–400 nm) were performed using a 10 mm path-length cuvette. Spectra were measured with 0, 8.6, 17.2, and 25.8  $\mu$ M hemin at 20°C, and averaged over 16 scans.

Dynamic light scattering (DLS) was performed at 25°C using a Zetasizer NanoS instrument (Malvern Instruments, Worcestershire, UK). Sample concentrations were adjusted to 0.47 mg/mL and 0.27 mg/mL for Bach1HBR-C wildtype (WT) and mCP, respectively. Measurements were conducted in triplicate. Data were analyzed with

the algorithms included in the Zetasizer Nano software.

#### Surface plasmon resonance

Experiments were performed on a BIAcore™ T200 instrument (GE Healthcare Life Sciences, Pittsburgh, PA, USA) with a Sensor Chip NTA (GE Healthcare Life Sciences). All analyses were performed at 25°C in HBS-N buffer (GE Healthcare Life Sciences) with 1 mM TCEP. For immobilization of ligand, the Sensor Chip NTA was activated with 0.5 mM NiCl<sub>2</sub> followed by capture of the C-terminal His<sub>6</sub>-tagged Bach1HBR-C. As the analyte, 1.25–20  $\mu$ M heme solution was injected. An untreated flow cell was used as a reference to correct for bulk response. Experiments were performed in duplicate. Dissociation constants ( $K_D$ ) were determined by fitting to a 1:1 interaction model, using the Biacore software (GE Healthcare Life Sciences). Stoichiometry was calculated based on the experimental  $R_{max}$  value, where stoichiometry =  $R_{max}/(MW_A/MW_L \times R_L)$  (A: analyte, L: ligand,  $R_L$ : immobilization level of ligand R).

A

```

Conf: 68888888899999997433358999999999942120000002456776346774047
Pred: CCCCCCCCCCCCCCCCCCCCCCCCCCCCCCCCCCHHHCCCCCCCCCHHHHHHCC
AA:  IGNYDYVSEPQQEPCPYACVISLGDSETDTEGDSESCSAREQDCEVKLPFFNAQRIISLS
      490          500          510          520          530          540

Conf: 768999998525995678788877531000356898532100001201578998553278
Pred: HHHHHHHHHHCCCCHHHHHHHHHHHHHHHHHHHHHHHHHHHHHHHHHHHHHHHHHH
AA:  RNDFQSLKMKHLTPQLDCIHDRRRSKNRIAAQRCRKRKLDLCIQNLESEIEKLQSEKE
      550          560          570          580          590          600

Conf: 888888889878865432344558997433049936787630158998773212467899
Pred: HHHHHHHHHHHHHHHHHHHHHHHHHHHHHHHHHHHHHHHHHHHHHHHHHHHHHHH
AA:  SLLKERDHIISTLGETKQNLGTGLCQQVCKEAALSPEQIQILAKYSASDCPLSFLISEKKGK
      610          620          630          640          650          660

Conf: 999998775544469999999999999997500000279998888876677776667
Pred: CCCCCCCCCCCCCCCCCCCCCCCCCCCCCCCCCCHHHCCCCCCCCCCCCCCCCCCCC
AA:  STPDGELAFTSVFSVDVPPPTAPPPCGRGSSAASQELVQESPPPTAAAPQATLLEPCRCQ
      670          680          690          700          710          720

Conf: 654233232234444799
Pred: CCCCCCCCCCCCCCCCCC
AA:  SAGISDFCQOMSDKCTTDE
      730
  
```

B

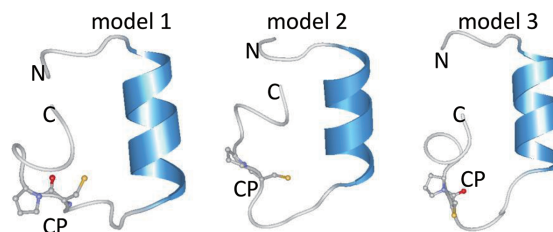


Fig. 2. Structure prediction of Bach1.

(A) The secondary structure elements for mouse Bach1 was predicted by PsiPred. The predicted result is shown for the C-terminal side of Bach1 (481–739). The predicted secondary structure elements are indicated H: helix, E: strand, and C: coil, respectively. The prediction confidence values are indicated from 0 (low) to 9 (high). The sequence included in this study is underlined (631–739). The functional CP motif (CP6) is boxed. (B) Predicted structures of the N-terminal peptide of Bach1HBR-C (SPEQIQILAKYSASDCPLSFLISEK). Helices are indicated by ribbon representations and the CP motifs are represented by a ball-and-stick model.

### Ultraviolet-visible spectroscopic analysis

Spectroscopic analyses were conducted as previously described (Watanabe-Matsui et al. 2011). To estimate heme binding, the UV-Vis spectroscopic measurements were performed at 20°C in 20 mM HEPES, pH 7.0, 50 mM NaCl. The sample cuvette contained 2  $\mu$ M each of Bach1HBR-C (WT or mCP) and bovine serum albumin (BSA), and the reference cuvette contained 40  $\mu$ M BSA only. Hemin was added to both the sample and reference cuvettes. In the sample cuvette, Bach1HBR-C bound heme preferentially, and excess heme bound to BSA. In the reference cuvette, the heme bound to BSA. Optical absorption spectra were recorded on a Lambda 45 spectrophotometer (Perkin Elmer, Waltham, US).

## Results and Discussion

### Secondary structure prediction and amino acid frequencies

Secondary structures can be predicted from the amino acid sequence with high accuracy (Yang et al. 2018), and this approach is good initial choice for structure determination of unknown proteins. In the present study, secondary structure prediction was performed using the PSIPRED server (Buchan et al. 2013). This approach (Jones 1999) predicted that the N-terminal region (635-642) of Bach1HBR-C would form a short helix (Fig. 2A). Analysis of amino acid frequency revealed that Bach1HBR-C contained high amounts of proline (11.0%) and serine (14.7%), which are enriched in the disordered region (Dunker et al. 2001). In addition, cysteine residues are included with high

frequency (4.6%) in compared with other proteins (Tompa 2002), which likely contribute to the function of Bach1 as a heme-binding protein.

### Heme binds to the CP motif

Heme binding was investigated using several experimental methods. Surface plasmon resonance analysis indicated that the dissociation constant ( $K_D$ ) and binding number for Bach1HBR-C WT with heme are  $1.37 \times 10^{-5}$  M and 2.3, respectively. The dissociation constant represents a relatively low affinity, and other heme-binding proteins exhibit  $K_D$  values from  $1 \times 10^{-6}$  M ( $\alpha$ 1-microglobulin) to  $1 \times 10^{-14}$  M (hemopexin) (Immenschuh et al. 2017). In our previous report, we found the  $K_D$  value for Bach2 with heme to be  $1.67 \times 10^{-7}$  M (Suenaga et al. 2016). The binding number of mCP with heme was not evaluated, as the affinity was likely to be very low and therefore may not be detectable.

Heme binding to proteins occurs via 5- and 6-coordination (Hira et al. 2007). We have previously reported that Bach2 can accept heme in these two binding modes in its intrinsically disordered region (Watanabe-Matsui et al. 2015). The UV-Vis spectroscopic analysis of the present study revealed two distinctive peaks at 365 and 428 nm in the spectrum of Bach1HBR-C WT (Fig. 3). These peaks relate to 5- and 6-coordinated heme binding, respectively (Hira et al. 2007). However, the mCP spectrum lacked the

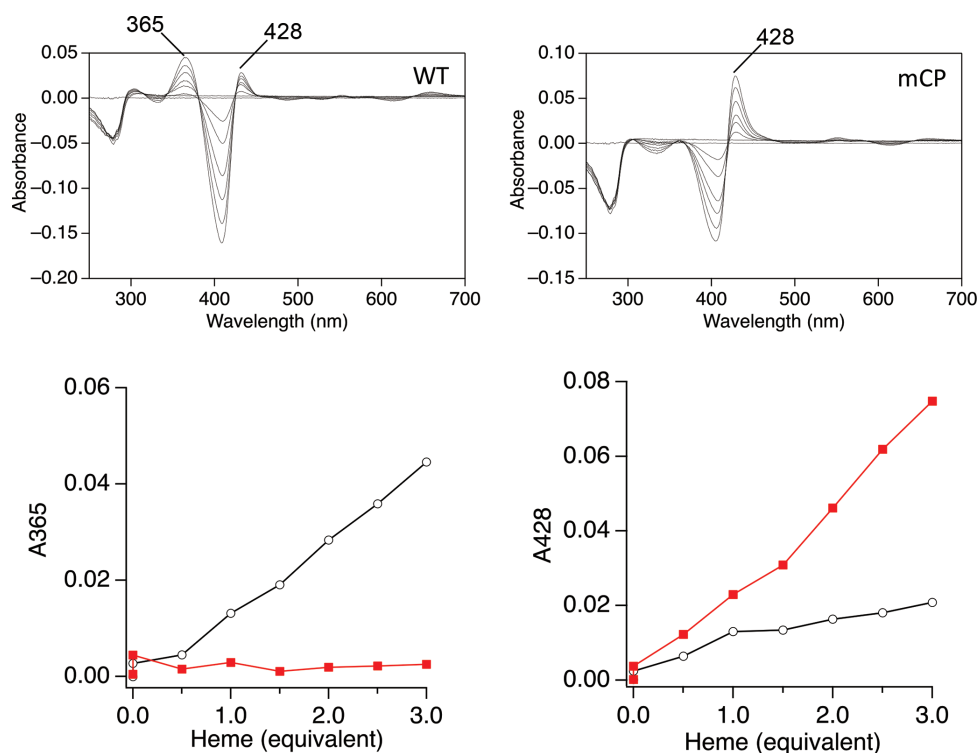


Fig. 3. Ultraviolet-Visible spectroscopic studies.

The difference absorption spectra for wild type (upper, left) and Cys649 mutant (upper, right) are shown. Absorption shifts at increasing heme concentrations are plotted for 364 nm (lower, left) and 428 nm (lower, right). The open circles and filled squares are indicated wild type and mutant, respectively. mCP, Cys649 to alanine mutated construct; WT, wild type.

peak at 365 nm (Fig. 3). The mCP mutant contains a single cysteine to alanine substitution at Cys649 in the CP motif; therefore, the CP motif can be concluded to be responsible for 5-coordinated heme binding. This finding is supported by previous reports (Hira et al. 2007). The CP motif-specific heme binding was also observed in the near-UV CD spectrum. The WT spectrum showed a gently-sloping positive peak around 320 nm (Fig. 4A) and a negative peak around 380 nm. Both peaks increased with increasing heme concentration. In contrast, mCP did not show any peaks in this region (Fig. 4B).

#### *Bach1HBR-C is intrinsically disordered*

CD spectrometry is commonly used to assess the secondary structure of proteins (Greenfield 2006). The spectrum in far UV region exhibits specific peaks for the secondary structures, and near-UV region include signals from such as aromatic amino acids, and are sensitive to the overall tertiary structure of the protein (Ranjbar and Gill 2009). The CD spectra in the far UV region (200–250 nm) are shown in Fig. 5. Spectra of both WT and mCP appear similar, and the addition of heme did not alter the spectra. In the present study, the similarities in the spectra of this region of WT and mCP samples indicated that the two were in similar conformational states. In addition, although heme bound to the two constructs through different binding

modes, this did not induce secondary structure changes in either.

DLS can be used to investigate the hydrodynamic radius of a protein molecule in solution. The hydrodynamic radius reflects the conformational state of a protein. The measured  $R_h$  values were 2.91 nm for WT and 2.75 nm for mCP, respectively. According to Uversky (2002),  $R_h$  can be estimated from the molecular mass for various sample states, including native (N), molten globule (MG), premolten globule (PMG), urea-unfolded (UU), guanidinium chloride (GdmCl)-unfolded (GU), natively unfolded-coil type (NU-coil), and natively unfolded-premolten globule type (NU-PMG). The molecular mass of Bach1HBR-C WT is 11,303.4 Da. The estimated  $R_h$  values for each protein state are shown in Table 1. Comparing these values with the measured  $R_h$  values shows good agreement with the NU-coil value, thus suggesting an intrinsically disordered protein.

#### *Heme binding does not induce helix formation*

To focus on the predicted short helix, we synthesized the N-terminal peptide of Bach1HBR-C, including one CP motif (SPEIQILAKYSASDCPLSFLISEK). De novo peptide structure prediction was possible for this sequence using PEP-FOLD 3 (Lamiable et al. 2016), which indicated ten predicted structures. Fig. 2B shows top three structures.

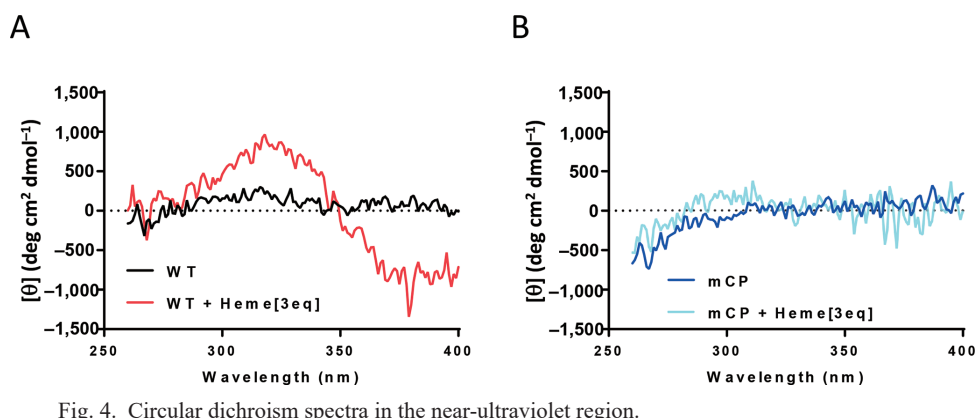


Fig. 4. Circular dichroism spectra in the near-ultraviolet region.

Circular dichroism spectra in the near-ultraviolet region for wild type (A) and mutant (B). mCP, Cys649 to alanine mutated construct; WT, wild type.

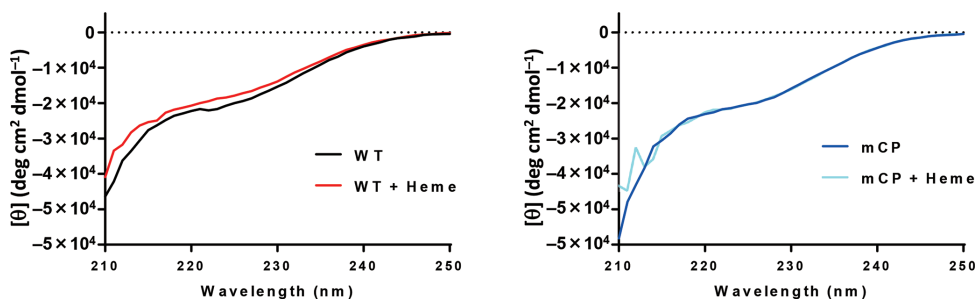


Fig. 5. Circular dichroism spectra in the far-ultraviolet region.

Circular dichroism spectra in the far-ultraviolet region for wild type (left) and mutant (right). mCP, Cys649 to alanine mutated construct; WT, wild type.



Table 1. Hydrodynamic radii estimation for various protein conformational states.

conformational state	N	MG	PMG	UU	GU	NU-coil	NU-PMG
$R_h$ (nm)	1.75	2.00	2.39	2.90	3.01	2.80	2.48

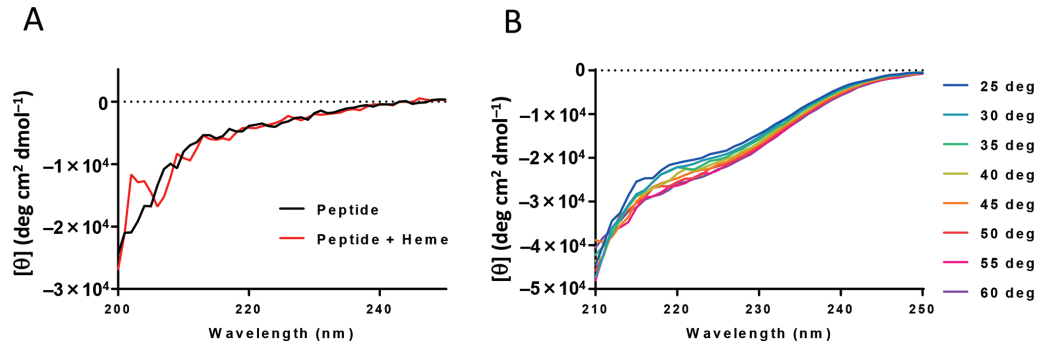


Fig. 6. Far-ultraviolet circular dichroism spectra.

(A) Spectra obtained for the synthesized peptide with/without heme. (B) Temperature shift of spectra obtained for Bach1HBR-C wild type.

mCP, Cys649 to alanine mutated construct; WT, wild type.

The prediction results suggested that the peptide forms a short helix at the N-terminal moiety, which is consistent with the results of secondary structure prediction. However, CD analysis of the peptide showed a decreasing curve with no peaks, similar to the spectrum of Bach1HBR-C (Fig. 6A). Furthermore, comparison of the curves without and with heme revealed that the addition of heme did not induce secondary structure, even though the CP motif is located in the vicinity of the predicted helix (Fig. 2B). When CD spectra of Bach1HBR-C WT were obtained at different temperatures (Fig. 6B), only a small shift was observed even when the temperature was increased up to 60°C. Definitive validation of the existence of secondary structure in this region is challenging, but the results presented here imply that there is either no helix or only a partial helix structure.

Changes in intrinsically disordered states have been observed as unstructured-structured transitions such as “encounter complex” or “coupled folding and folding” (Shammas et al. 2016). These proteins/regions exist in an unfolded or partially-structured state, transitioning to a structured form upon binding with their partners. The complex formed by the phosphorylated kinase-inducible domain and the kinase interacting domain (the pKID-KIX complex) is one such complex (Sugase et al. 2007). Alone, the pKID domain adopts an unstructured conformation in solution, forming  $\alpha$ -helices upon binding with KIX. Secondary structure prediction using PSIPRED or PEP-FOLD suggests the existence of helices, which have been confirmed in the crystal structure (Radhakrishnan et al. 1997). The predicted structure of Bach1HBR-C suggests similarities, in that helices are predicted; however, no structure was detected with biophysical analyses in this case. Although it is the native binding partner of Bach1HBR-C, our results

indicate that heme cannot be the trigger for conformational transition. The Bach1-heme system must, therefore, have a distinctive regulation strategy as an intrinsically disordered protein. A number of potential binding partners have been suggested for Bach1 (Li et al. 2018), and so the unstructured-structured transition of Bach1 may be induced by other binding partners.

### Conclusions

In this study, the Bach1 C-terminal heme-binding region was analyzed using biophysical techniques. This region was found to be intrinsically disordered, and able to accept heme in 5- and 6-coordination binding modes. The CP motif is responsible for 5-coordinated heme binding, as has been shown in Bach2. The conformational state of Bach1HBR-C did not change upon the addition of heme, and no biological response in terms of unstructured-structured transition was observed. We therefore conclude that Bach1HBR-C does not undergo unstructured-structured transition with heme; instead, the heme response of the region occurs through a disorder-disorder conformational alteration.

### Acknowledgments

We acknowledge the support of the Biomedical Research Core of the Tohoku University Graduate School of Medicine. This work was supported by a JSPS Grant-in-Aid for Scientific Research Number 18H04021 and 15H02506 (K.I.) and Research Fellowships for Young Scientists (grant number 16J40189) and Grant-in-Aid for Scientific Research 16K08573 to M. W.-M. We thank Amy Phillips, Ph.D., from Edanz Group (<https://www.edanzediting.com/>) for editing a draft of this manuscript.

### Author Contributions

K.S., M.W.-M. and K.M. performed experimental studies.

T.M. and K.I. supervised the experiments. K.S. and K.M. wrote the manuscript.

### Conflict of Interest

The authors declare no conflict of interest. However, K.I. and K.M. received partial financial support from Teijin Pharma Co., Ltd. through a collaborative research contract.

### References

- Buchan, D.W., Minneci, F., Nugent, T.C., Bryson, K. & Jones, D.T. (2013) Scalable web services for the PSIPRED protein analysis workbench. *Nucleic Acids Res.*, **41**, W349-357.
- Chung, S.W., Hall, S.R. & Perrella, M.A. (2009) Role of haem oxygenase-1 in microbial host defence. *Cell. Microbiol.*, **11**, 199-207.
- Dunker, A.K., Lawson, J.D., Brown, C.J., Williams, R.M., Romero, P., Oh, J.S., Oldfield, C.J., Campen, A.M., Ratliff, C.M., Hipps, K.W., Ausio, J., Nissen, M.S., Reeves, R., Kang, C., Kissinger, C.R., et al. (2001) Intrinsically disordered protein. *J. Mol. Graph. Model.*, **19**, 26-59.
- Greenfield, N.J. (2006) Using circular dichroism spectra to estimate protein secondary structure. *Nat. Protoc.*, **1**, 2876-2890.
- Hintze, K.J., Katoh, Y., Igarashi, K. & Theil, E.C. (2007) Bach1 repression of ferritin and thioredoxin reductase1 is heme-sensitive in cells and in vitro and coordinates expression with heme oxygenase1, beta-globin, and NADP(H) quinone (oxido) reductase1. *J. Biol. Chem.*, **282**, 34365-34371.
- Hira, S., Tomita, T., Matsui, T., Igarashi, K. & Ikeda-Saito, M. (2007) Bach1, a heme-dependent transcription factor, reveals presence of multiple heme binding sites with distinct coordination structure. *IUBMB life*, **59**, 542-551.
- Igarashi, K. & Watanabe-Matsui, M. (2014) Wearing red for signaling: the heme-bach axis in heme metabolism, oxidative stress response and iron immunology. *Tohoku J. Exp. Med.*, **232**, 229-253.
- Immenschuh, S., Vijayan, V., Janciauskiene, S. & Gueler, F. (2017) Heme as a target for therapeutic interventions. *Front. Pharmacol.*, **8**, 146.
- Ishikawa, M., Numazawa, S. & Yoshida, T. (2005) Redox regulation of the transcriptional repressor Bach1. *Free Radic. Biol. Med.*, **38**, 1344-1352.
- Ito, N., Watanabe-Matsui, M., Igarashi, K. & Murayama, K. (2009) Crystal structure of the Bach1 BTB domain and its regulation of homodimerization. *Genes Cells*, **14**, 167-178.
- Jones, D.T. (1999) Protein secondary structure prediction based on position-specific scoring matrices. *J. Mol. Biol.*, **292**, 195-202.
- Lamiable, A., Thevenet, P., Rey, J., Vavrusa, M., Derreumaux, P. & Tuffery, P. (2016) PEP-FOLD3: faster de novo structure prediction for linear peptides in solution and in complex. *Nucleic Acids Res.*, **44**, W449-454.
- Lathrop, J.T. & Timko, M.P. (1993) Regulation by heme of mitochondrial protein transport through a conserved amino acid motif. *Science*, **259**, 522-525.
- Li, J., Shima, H., Nishizawa, H., Ikeda, M., Brydun, A., Matsumoto, M., Kato, H., Saiki, Y., Liu, L., Watanabe-Matsui, M., Iemura, K., Tanaka, K., Shiraki, T. & Igarashi, K. (2018) Phosphorylation of BACH1 switches its function from transcription factor to mitotic chromosome regulator and promotes its interaction with HMMR. *Biochem. J.*, **475**, 981-1002.
- Radhakrishnan, I., Perez-Alvarado, G.C., Parker, D., Dyson, H.J., Montminy, M.R. & Wright, P.E. (1997) Solution structure of the KIX domain of CBP bound to the transactivation domain of CREB: a model for activator:coactivator interactions. *Cell*, **91**, 741-752.
- Ranjbar, B. & Gill, P. (2009) Circular dichroism techniques: biomolecular and nanostructural analyses: a review. *Chem. Biol. Drug Des.*, **74**, 101-120.
- Rosbrook, G.O., Stead, M.A., Carr, S.B. & Wright, S.C. (2012) The structure of the Bach2 POZ-domain dimer reveals an intersubunit disulfide bond. *Acta Crystallogr. D Biol. Crystallogr.*, **68**, 26-34.
- Shammas, S.L., Crabtree, M.D., Dahal, L., Wicky, B.I. & Clarke, J. (2016) Insights into coupled folding and binding mechanisms from kinetic studies. *J. Biol. Chem.*, **291**, 6689-6695.
- Suenaga, T., Watanabe-Matsui, M., Uejima, T., Shima, H., Matsui, T., Ikeda-Saito, M., Shirouzu, M., Igarashi, K. & Murayama, K. (2016) Charge-state-distribution analysis of Bach2 intrinsically disordered heme binding region. *J. Biochem.*, **160**, 291-298.
- Sugase, K., Dyson, H.J. & Wright, P.E. (2007) Mechanism of coupled folding and binding of an intrinsically disordered protein. *Nature*, **447**, 1021-1025.
- Sun, J., Hoshino, H., Takaku, K., Nakajima, O., Muto, A., Suzuki, H., Tashiro, S., Takahashi, S., Shibahara, S., Alam, J., Taketo, M.M., Yamamoto, M. & Igarashi, K. (2002) Hemoprotein Bach1 regulates enhancer availability of heme oxygenase-1 gene. *EMBO J.*, **21**, 5216-5224.
- Suzuki, H., Tashiro, S., Hira, S., Sun, J., Yamazaki, C., Zenke, Y., Ikeda-Saito, M., Yoshida, M. & Igarashi, K. (2004) Heme regulates gene expression by triggering Crml-dependent nuclear export of Bach1. *EMBO J.*, **23**, 2544-2553.
- Tomba, P. (2002) Intrinsically unstructured proteins. *Trends Biochem. Sci.*, **27**, 527-533.
- Uversky, V.N. (2002) What does it mean to be natively unfolded? *Eur. J. Biochem.*, **269**, 2-12.
- Watanabe-Matsui, M., Matsumoto, T., Matsui, T., Ikeda-Saito, M., Muto, A., Murayama, K. & Igarashi, K. (2015) Heme binds to an intrinsically disordered region of Bach2 and alters its conformation. *Arch. Biochem. Biophys.*, **565**, 25-31.
- Watanabe-Matsui, M., Muto, A., Matsui, T., Itoh-Nakadai, A., Nakajima, O., Murayama, K., Yamamoto, M., Ikeda-Saito, M. & Igarashi, K. (2011) Heme regulates B-cell differentiation, antibody class switch, and heme oxygenase-1 expression in B cells as a ligand of Bach2. *Blood*, **117**, 5438-5448.
- Yamada, K., Tanaka, N., Nakanishi, K., Kamei, N., Ishikawa, M., Mizuno, T., Igarashi, K. & Ochi, M. (2008) Modulation of the secondary injury process after spinal cord injury in Bach1-deficient mice by heme oxygenase-1. *J. Neurosurg. Spine*, **9**, 611-620.
- Yang, Y., Gao, J., Wang, J., Heffernan, R., Hanson, J., Paliwal, K. & Zhou, Y. (2018) Sixty-five years of the long march in protein secondary structure prediction: the final stretch? *Brief. Bioinform.*, **19**, 482-494.
- Yano, Y., Ozono, R., Oishi, Y., Kambe, M., Yoshizumi, M., Ishida, T., Omura, S., Oshima, T. & Igarashi, K. (2006) Genetic ablation of the transcription repressor Bach1 leads to myocardial protection against ischemia/reperfusion in mice. *Genes Cells*, **11**, 791-803.
- Zhang, L. & Guarente, L. (1995) Heme binds to a short sequence that serves a regulatory function in diverse proteins. *EMBO J.*, **14**, 313-320.